High-Temperature Latent Heat Storage Technology to Utilize Exergy of Solar Heat and Industrial Exhaust Heat

Takahiro Nomura and Tomohiro Akiyama

1 Introduction

To utilize the exergy of solar and industrial exhaust heat, high-temperature thermal energy storage (TES) systems are required, which can effectively store the intermittent high-temperature heat of such sources. Recently, development of an advanced TES system with high heat storage capacity and high thermal responsivity was accelerated because conventional sensible heat storage (SHS) systems using ceramics, bricks, and liquid molten salts have low heat storage capacity and low thermal responsivity. Under these circumstances, latent heat storage (LHS) technology has attracted considerable attention. LHS is based on the storage or release of latent heat when a phase change material (PCM) undergoes phase transition from solid to liquid, or vice versa. LHS has three advantages: its latent heat provides high heat storage capacity compared to SHS, it can be a constant heat source at the phase-changing temperature during the phase transition, and the reversible phase-changing process allows for repeated use (Nomura et al. 2013).These advantages allow LHS to be used as an advanced TES system, instead of SHS. In this article, general LHS technology is outlined first; then recent advances in the use of LHS for high-temperature applications (over 100 °C) are discussed, with respect to each type of PCM (e.g., sugar alcohol (Kojima and Matsuda, 2004), molten salt, and alloys). In addition, the prospects for future LHS technology are discussed from the viewpoint of exergy.

T. Nomura (✉) • T. Akiyama
Center for Advanced Research of Energy and Materials, Hokkaido University, Kita 13 Nishi 8, Kita-ku, Sapporo 060-8628, Japan
e-mail: nms-tropy@eng.hokudai.ac.jp

Nomenclature

| A	Energy level ($-$)
C_P	Specific heat ($J \cdot g \cdot K^{-1}$)
$C_{P,l}$	Specific heat of liquid ($J \cdot g \cdot K^{-1}$)
$C_{P,s}$	Specific heat of solid ($J \cdot g \cdot K^{-1}$)
$\Delta h_{T_o}^0$	Enthalpy change of a chemical reaction under standard condition ($J \cdot mol^{-1}$)
L	Latent heat ($J \cdot g^{-1}$)
m	Mass (g)
Q	Quantity of heat (J)
$\vec{Q} \rightarrow$	Vector of heat source
$\vec{R} \rightarrow$	Vector of reaction
T	Temperature (°C)
T_0	Reference temperature (°C)
T_m	Melting point (°C)
ε	Exergy ($J \cdot g^{-1}$)
ε_L	Exergy of latent heat ($J \cdot g^{-1}$)
$\Delta \varepsilon_{T_o}^0$	Exergy change of a chemical reaction under standard condition ($J \cdot mol^{-1}$)
Abbreviation	
CSP	Concentrated solar power
DSG	Direct steam generator
HTF	Heat transfer fluid
LHS	Latent heat storage
PCM	Phase change material
SHS	Sensible heat storage
TES	Thermal energy storage

2 Principle of LHS

Figure 1 illustrates the differences between LHS using solid–liquid phase transition, and SHS. Here, the specific heat of PCM and SHS materials was constant. The cumulative heat storage capacity of SHS was

$$Q = mC_P(T - T_i) \tag{1}$$

Here, Q is quantity of heat, m is weight of heat storage material, C_p is a specific heat, T is temperature, and T_i is initial temperature. In the SHS, the phases of the material do not change. On the other hand, Q of LHS was as follows:

$$Q = m\{C_{P,l}(T - T_m) + L + C_{P,s}(T_m - T_i)\} \tag{2}$$

Fig. 1 Difference of
cumulative heat storage
capacity of LHS using
solid–liquid phase transition
and SHS
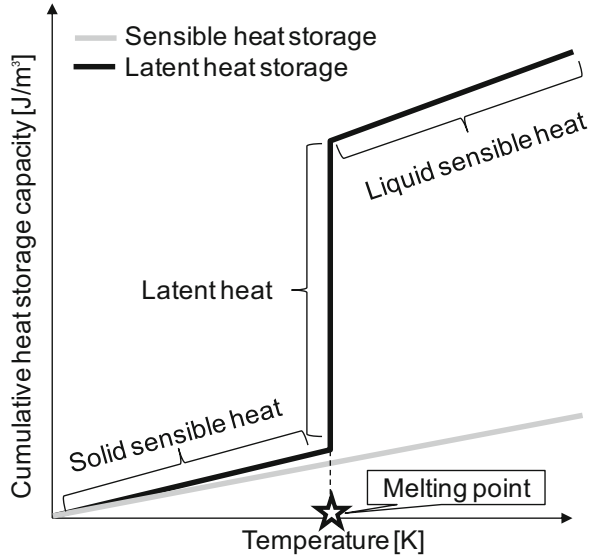
Here, $C_{P,l}$ is liquid sensible heat, $C_{P,s}$ is solid sensible heat, T_m is melting point, and L is latent heat. LHS stores/releases thermal energy when it changes phase; therefore, Q drastically changes at T_m. This simple principle provides high heat capacity, the function of use as an isothermal heat source, and repeatable use.

3 Heat Exchanger for LHS

Figure 2 shows the classification of LHS heat exchangers. Packed-bed, shell-and-tube, fluidized bed, and direct-contact type have been proposed. The packed-bed type and shell-and-tube type are classified as indirect-passive heat exchangers: heat exchange proceeds through a heat transfer wall between the PCM and the heat transfer fluid (HTF). A packed-bed heat exchanger using PCM capsules has advantages such as quick thermal response and high heat storage density, due to a large area of heat transfer. The advantages of the shell and tube type are that high-pressure steam can be used as HTF, only considering the high-pressure design of the heat transfer tubes. Fluidized bed designs are classified as indirect-active heat exchangers: heat is exchanged through a heat transfer wall between the PCM and the HTF. Here, not only the HTF but also the PCM is circulated in the heat storage system. The fluidized bed type can transport dense thermal energy from one process to another. Combination of the PCM with liquid (Yamagishi et al. 1999) or gas (Izquierdo-Barrientos et al. 2013) as the HTF was proposed. The other type is a direct-contact heat exchanger: the heat exchange proceeds between the PCM and the HTF without any heat transfer wall. Here, the PCM is required to be insoluble in the heat transfer medium, and the density of the PCM is required to be high enough
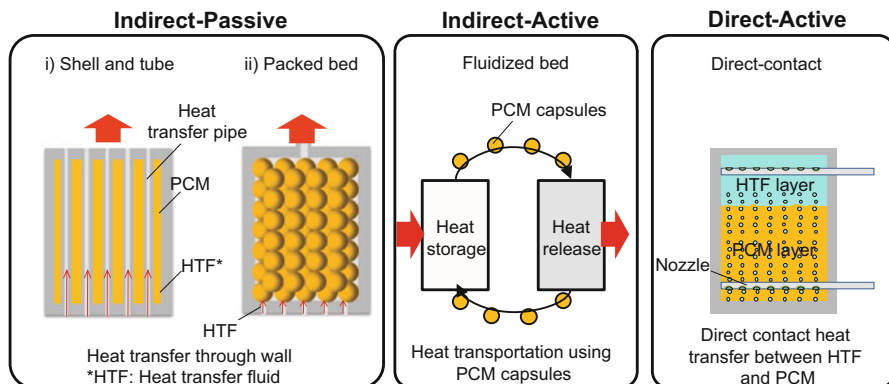
Fig. 2 Classification of heat exchangers for LHS

to ensure that a phase separation is possible. The direct-contact heat exchanger has a very simple, light structure and a high thermal storage density. This is because only the inlet and outlet nozzles are required for the HTF, and a heat transfer pipe and capsule are not required. Therefore, this process can be carried out using not only a stationary system but also a heat transport system (Kaizawa et al. 2008a).

4 Recent Advances of High-Temperature PCM

Figure 3 shows the relationship between T_m and latent heat of common high-temperature PCM candidates. Among these high-temperature candidates are sugar alcohol, molten salt, and alloy. The T_m of each material clearly involves a specific temperature range. The T_m of sugar alcohols is under 200 °C, molten salt is mainly over 300 °C, and alloy is over 500 °C. Therefore, in this section, the recent advances in the use of LHS for high-temperature applications will be discussed for each type of PCM candidate: sugar alcohol, molten salt, and alloy.

4.1 Sugar Alcohols ($T_m < 200$ °C)

Sugar alcohols are promising PCM candidates for utilizing thermal energy at 100–200 °C. Table 1 lists the thermophysical properties of sugar alcohol PCMs (Hidaka et al. 2000; Kaizawa et al. 2008b). In this section, the advantages, problems, and prospects of sugar alcohol PCMs are presented.

Advantages High heat storage density is a major advantage of sugar alcohols. As shown in Table 1, single component sugar alcohols have large latent heat (over 250 J·g^{-1}). The latent heats of erythritol, mannitol, and galactitol are as large as the

Fig. 3 Relationship between T_m and latent heat of high-temperature PCM candidates
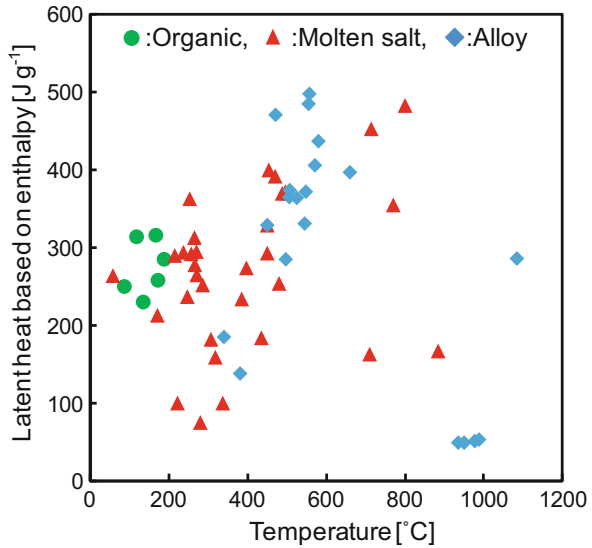

Table 1 Thermophysical properties of sugar alcohol PCMs

Material	T_m [°C]	L [J g^{-1}]
D-threitol	87	250
Erythritol	118	314
High-density polyethelene	135	230
D-mannitol	167	316
Hydroquinone	172	258
Pentaerythritol	188	285

latent heat of the solid–liquid phase change of water. Other advantages of sugar alcohols are that they are nontoxic and inflammable. Typical applications of sugar alcohols involve foods and food additives. In addition, the sugar alcohols do not cause chemical corrosion of the metals used as the heat transfer wall.

Disadvantages The low thermal conductivity of typical sugar alcohols is the most serious problem in using them as PCMs. For example, the thermal conductivity of the typical sugar alcohol PCM, erythritol (T_m: 118 °C, latent heat: 314 J·g^{-1}) (Kakiuchi et al. 1998) is 0.73 W·m^{-1}·K^{-1} (Oya et al. 2013). Therefore, methods to enhance the effective thermal conductivity of the sugar alcohol PCMs have been widely studied (Liu et al. 2012). Another problem related to use of sugar alcohol PCMs, is that they have less thermal endurance. Sugar alcohols with T_m over 150 °C have been reported, but their thermal endurance was too low to use for long periods (Nomura et al. 2015a).

Applications and Recent Studies The LHS systems using sugar alcohol PCMs do have practical uses. Here, a latent heat transportation (LHT) system will be introduced. In this system, a mobile latent heat accumulator recovers industrial exhaust

heat and distributes it over wide areas located at distances up to 35 km from the heat source. The industrial exhaust heat is compactly stored in the form of latent heat by melting the PCMs, which are then transported by truck to places such as office buildings, hospitals, and hotels, (Kaizawa et al. 2008a). Erythritol was used as PCM for the LHT system due to its large latent heat, and its suitability (T_m 118 °C) for recovery of low-temperature industrial exhaust heat. In addition, this T_m is high enough to operate a single effect absorption chiller that supplies cold water at about 5–7 °C. This heat transfer system has been applied commercially in Japan. A 20 t heat transfer container is used in the practical system, and each container can supply 1.3 MWh of thermal energy per cycle.

Future Work There is a strong need to develop and utilize new sugar alcohol PCMs with T_m around 150 °C. This is because a PCM with T_m around 150 °C could produce low-pressure steam and operate double or triple effect absorption chillers, of which the coefficient of performance is over 1.0. Although sugar alcohol PCM candidates with T_m around 150 °C, such as mannitol have been reported, and pilot-scale heat exchange experiments were performed (Gil et al. 2013), they have low thermal stability (Sagara et al. 2014). Therefore, the enhancement of the thermal stability of sugar alcohol PCMs is expected.

4.2 Molten Salt ($T_m > 300$ °C)

Molten salts (e.g., nitrates, carbonates, and chlorides) are the most common high-temperature PCMs for use of thermal energy sources at over 300 °C. Table 2 lists the thermophysical properties of the molten salt PCMs (Guillot et al. 2012; Nomura et al. 2010; Japan Society of Thermophysical Properties 2008). In this section, the advantages, problems, and prospects for the uses of molten salt PCMs, are presented.

Advantages High heat storage density is a great advantage of molten salt PCMs. Generally, molten salts are low cost; therefore, they have also high heat storage capacity per unit cost. As shown in Table 2, many molten salts can function as PCMs, therefore, molten salt PCMs can be used in a variety of systems.

Disadvantages The molten salt PCMs have three serious disadvantages. First is low thermal conductivity: the thermal conductivity of typical molten salt PCMs is under 1 W m^{-1} K^{-1}. Second is their high volume expansion ratio during phase transition: the volume of expansion makes it difficult to design PCM capsules or heat storage units because the thermal stress from the volume expansion breaks the heat transfer wall and shell of the PCM capsules. For example, the volume expansion ratio of NaCl (T_m: 800 °C), the most often used molten salt PCM, is 0.26 (Japan Society of Thermophysical Properties 2008). Third is their high level of chemical corrosion: liquid molten salts generally exhibit high levels of chemical corrosion of metallic shell materials.

Table 2 Thermophysical properties of molten salt PCMs

PCM	T_m [°C]	L [J g^{-1}]
NaNO$_3$-KNO$_3$ (46–54 wt%)	222	100
NaOH-NaNO$_3$ (28–72 mol%)	247	237
NaOH-NaNO$_3$ (81.5–18.5 mol%)	257	292
NaOH·NaNO$_2$	265	313
NaOH-NaNO$_3$ (59–41 mol%)	266	278
2NaOH·NaNO$_3$	270	295
NaOH·NaNO$_3$	271	265
NaOH-Na$_2$CO$_3$(82.9–17.1 wt%)	286	252
NaNO$_3$	307	182
NaOH	318	159
KNO$_3$	337	100
NaCl-KCl-MgCl$_2$ (33.0–21.6–45.4 mol%)	385	234
NaCl-MgCl$_2$ (60.1–39.9 mol%)	450	293
2KCl-MgCl$_2$ (42.0–58.0 mol%)	470	392
Na$_2$CO$_3$-K$_2$CO$_3$ (59–41 mol%)	710	163
MgCl$_2$	714	453
KCl	770	355
NaCl	800	483
Na$_2$CO$_3$	858	258

Applications and Recent Studies TES plays a vital role in concentrated solar power (CSP) plants because it is subjected to the intermittencies of the source and to the difficulties of matching electrical needs with the availability of solar insolation (Guillot et al. 2012). Although SHS using liquid molten salt has been applied in some presently operating commercial CSP plants, a great deal of salt is required, for examples 28,500 t of KNO$_3$-NaNO$_3$ for generating only 50 MW × 7.5 h/day (Rellso and Delgado 2009). Therefore, recent development of an LHS system using nitric acid as the PCM for CSP facilities has been accelerating. In particular, the shell and tube type heat exchanger, which can serve as a direct steam generator (DSG), is a promising system (Bayón et al. 2010) for this use.

Bayón et al. (2010) reported a DSG demonstration experiment using a 100 kWth plant using a PCM composite of graphite/eutectic mixtures of KNO$_3$-NaNO$_3$. Graphite was mixed in to enhance the effective thermal conductivity of the KNO$_3$-NaNO$_3$. Laing et al. (2011) proposed a hybrid heat exchange system using concrete SHS and sodium salt LHS. In addition, a packed bed heat exchanger using PCM capsules, which could easily expand the heat transfer area, was also reported. Mathur et al. (2013) developed new PCM capsules of about 5 mm diameter.

Future Work The work on the LHS system using nitric acids (T_m about 300 °C) is in validation phase (Bayón et al. 2010). On the other hand, innovations in CSP solar receivers, from troughs to central towers, have increased the concentrated temperature. Therefore, development of an LHS system using a molten salt PCM with T_m up to 1000 °C is expected.

4.3   *Metal Alloys* ($T_m > 500\ °C$)

Using metal alloys for high-temperature PCMs has many advantages. Table 3 lists the thermophysical properties of alloys as PCM candidates (Kenisarin 2010; Maruoka and Akiyama 2006). In this section, the advantages, problems, and prospects of metal alloy PCMs are presented.

Advantages   The heat storage capacity of alloys is as high as that of the molten salt PCMs. In addition, the latent heat, based on volume of alloy, is larger than that of molten salt, since the density of alloys is generally higher than that of molten salt. Therefore, more compact LHS alloy systems can be designed than for systems using molten salt PCM. The high thermal conductivity of alloys is their most critical advantage. For example, the thermal conductivity of Al is 400 times greater than that of $NaNO_3$. The low volume expansion ratio of alloys during phase transition is also a great advantage since it makes the design of LHS easier.

Disadvantages   Liquid metal alloys generally exhibit high chemical corrosion of metallic shell materials. This is the most serious problem regarding the use of metallic PCMs. To use them, ceramics must be applied over the structural materials used to build the heat storage units and shells of capsules.

Recent Studies   The use of metallic PCM for LHS is promising for effective use of high-temperature thermal energy, but development of this technology has just started. Thus, no large-scale experiments have been conducted, as far as is known. The development of materials and heat exchanger designs has been reported. The development of high-temperature LHS technologies based on Al-Si series PCMs, in particular, is accelerating. Nomura et al. (2014) have proposed a

Table 3 Thermophysical properties of metallic PCMs

PCM	T_m [°C]	L [J g^{-1}]
Mg-Zn (46.2–53.7 wt%)	340	185
Zn-al (96–4 wt%)	381	138
Al-Si-Sb (86.4–9.4–4.2 wt%)	471	471
Mg-al (34.65–65.35 wt%)	497	285
Al-cu-mg (60.8–33.2–6.0 wt%)	506	365
Al-Si-cu-mg (64.1–5.2–28–2.2 wt%)	507	374
Al-Si-cu (68.5–5.0–28–26.5 wt%)	525	364
Al-cu-Sb (64.3–5.0–34.0–1.7 wt%)	545	331
Al-cu (66.92–33.08 wt%)	548	372
Al-Si-mg (83.14–11.7–5.16 wt%)	555	485
Al-Si (87.76–12.24 wt%)	557	498
Al-Si (75–25 wt%)	557	437
Al-Si-cu (46.3–4.6–49.1 wt%)	571	406
Al	660	330
Cu-Si (80–20 wt%)	802	197
Cu	1084	286

high-temperature PCM base on an Al-Si series alloy (T_m over 500 °C). The heat storage capacity of this Al-Si series PCM was about 1.5-times higher than that of $MgCl_2$ (a typical molten salt PCM). Kotze et al. (2014) proposed a shell-and-tube-type heat exchanger, in which Al-12wt%Si was used as a PCM, and NaK was used as the HTF. In addition, a super-high-temperature PCM (above 1000 °C) has also been reported. Maruoka and Akiyama (2006) proposed a core-shell-type PCM macrocapsule using a Cu core and Ni shell, achieved using an electroplating method. This PCM capsule has hybrid functions: thermal energy storage and catalyst. This encapsulation method is being refined (Zhang et al. 2014).

5 Discussion

In this section, the prospects for future LHS technology are discussed from the viewpoint of exergy.

Figure 4 shows the relationship between energy level (indicating energy quality), and exergy (latent heat) of the high-temperature PCM candidates. Here, the energy levels of PCMs (at T_m) and their exergy are defined as follows:

$$A = \frac{(T_m - T_0)}{T_m} \tag{3}$$

and

Fig. 4 Relationship between energy level and exergy of latent heat of these materials
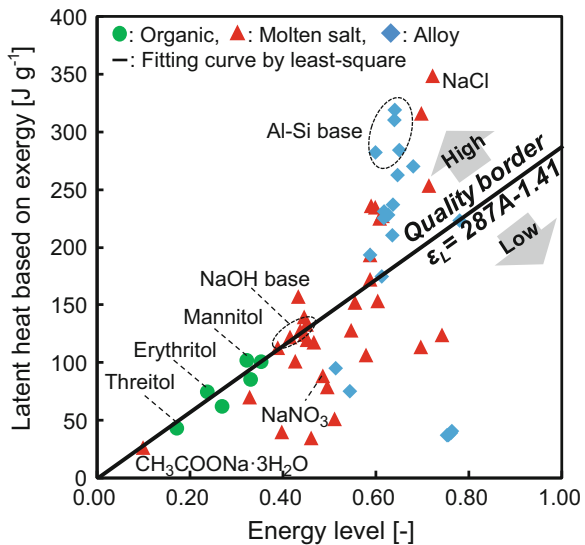
$$\varepsilon_{\mathrm{L}} = AL \qquad (4)$$

Here, A is energy level, ε_{L} is exergy of latent heat, and T_0 is environmental temperature (298.15 K).

By considering the relationship between A and ε_{L}, the PCMs that should be focused upon can be determined. The line in Fig. 4 was a least square fitting of the plots. Interestingly, the PCMs that are used commercially, or near practical use (e.g., $CH_3COONa \cdot 3H_2O$, threitol, erythritol, mannitol, and molten salt of NaOH-series) were almost on the line. Therefore, the PCMs on the line could be classified as good quality PCMs (adequate for practical use). The PCMs under the line were lower quality PCMs, and therefore, should not be selected, except for special reasons. From this viewpoint, $NaNO_3$ or $NaNO_3$-KNO_3 should not be selected as PCM. However, they have been used in many studies (Acem et al. 2010; Pacheco et al. 2002; Pincemin et al. 2008) about LHS systems. This is because only the $NaNO_3$ does not corrode structural materials, among the molten salt PCMs, for the temperature range of about 300 °C. The PCM candidates above the line, including the Al-Si series and NaCl, were classified as high-quality PCMs. Although there are few studies about these high-quality PCMs, the future development of LHS, with respect to exergy, should be focused upon them.

Focusing on the application of LHS, conversion of PCM thermal energy to chemical energy (e.g., hydrogen) using endothermic reactions has advantages since thermal exergy at low energy levels can be recuperated to chemical exergy at high energy levels (Tsutumi and Yoshida 1999). Here, the exergy recuperation (Tsutsumi 2004) concept will be introduced using the method called 'thermodynamic compass' (Ishida 2002). This is a graphic method developed by M. Ishida (2002) that can express every process and synthesis as vectors in two-dimensional space with X-axis of enthalpy change ΔH, and Y-axis of exergy change $\Delta \varepsilon$. In evaluating a system thermodynamically, summations of ΔH and $\Delta \varepsilon$ in each process are restricted by the first and second laws of thermodynamics, as expressed in the following equations:

First law of thermodynamics:

$$\sum \Delta H = 0 \qquad (5)$$

Second law of thermodynamics:

$$\sum \Delta \varepsilon = 0 \qquad (6)$$

For each vector in a process, the ratio of $\Delta \varepsilon$ to ΔH gives the slope, called the energy level, A, indicating energy quality.

A vector and energy level for a chemical reaction can be expressed by the following equation:

$$\vec{R} = (\Delta H, \Delta \varepsilon) = \left(\Delta h_{T_o}^0, \Delta \varepsilon_{T_o}^0 \right) \tag{7}$$

$$A = \frac{\Delta \varepsilon_{T_o}^0}{\Delta h_{T_o}^0} \tag{8}$$

Here, $\vec{R} \rightarrow$, $\Delta h_{T_o}^0$, and $\Delta \varepsilon_{T_o}^0$ mean vector, enthalpy change, and exergy change of a chemical reaction at standard temperature T_0 (298.15 K) and standard pressure (1 atm). A vector and energy level for a heat source at T, with enthalpy of Q, can be expressed by the following equation:

$$\vec{Q} = (\Delta H, \Delta \varepsilon) = (Q, AQ) \tag{9}$$

$$A = \frac{T - T_0}{T} \tag{10}$$

Here, $\vec{Q} \rightarrow$ is a vector of the heat source.

To promote the efficient utilization of energy, the system should have a shorter resultant vector.

Figure 5 shows synthesis of a vector of dry reforming of CH_4 to produce 2 mol of syngas ($CO:H_2 = 1:1$ mol) and a basic heat source on the thermodynamics compass. The reaction equation, vector, and energy level of dry reforming of CH_4, which is an endothermic reaction, is expressed as

$$\vec{R}_{reforming}$$
$$CH_4 + CO_2 \rightarrow 2H_2 + 2CO \tag{11}$$
$$(\Delta H, \Delta \varepsilon) = (0.247, 0.171) \tag{12}$$
$$A = 0.69 \tag{13}$$

Here, $\vec{R}_{reforming}$ is a vector for dry reforming of CH_4.

Due to thermodynamic restrictions, a heat source at 690 °C must be provided in a support process.

$$\vec{Q}_{reforming}$$
$$(\Delta H, \Delta \varepsilon) = (-0.247, -0.171) \tag{14}$$
$$A = 0.69, \quad T = 690°C \tag{15}$$

Here, $\vec{Q}_{reforming}$ is a vector of the heat source for dry reforming. As results, the following relationship was established:
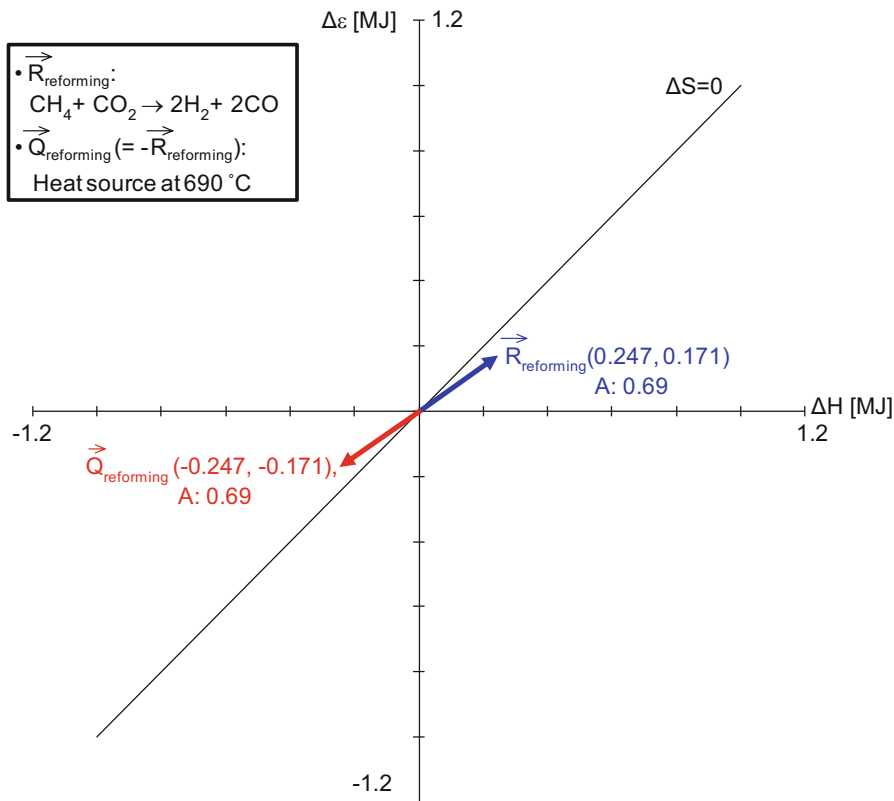
Fig. 5 Synthesis of a vector for dry reforming of CH_4 to produce 2 mol of syngas and a basic heat source

$$\overrightarrow{Q}_{\text{reforming}} = -\overrightarrow{R}_{\text{reforming}} \tag{16}$$

As discussed before, the dry reforming of CH_4 produces 2 mol of syngas by the combination of 1 mol of CH_4 and heat source at 690 °C. The chemical energy of CH_4 and syngas can be expressed on the thermodynamic compass as a perfect combustion reaction of each material:
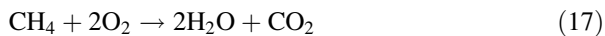
$$\overrightarrow{R_{\text{CH4}}}$$
$$CH_4 + 2O_2 \rightarrow 2H_2O + CO_2 \tag{17}$$
$$(\Delta H, \Delta \varepsilon) = (-0.891, -0.818) \tag{18}$$

$$A = 0.92 \tag{19}$$

Fig. 6 Relationship of $\vec{R}_{CH4}$, $\vec{R}_{syngas}$, $\vec{R}_{reforming}$, and $\vec{Q}_{reforming}$
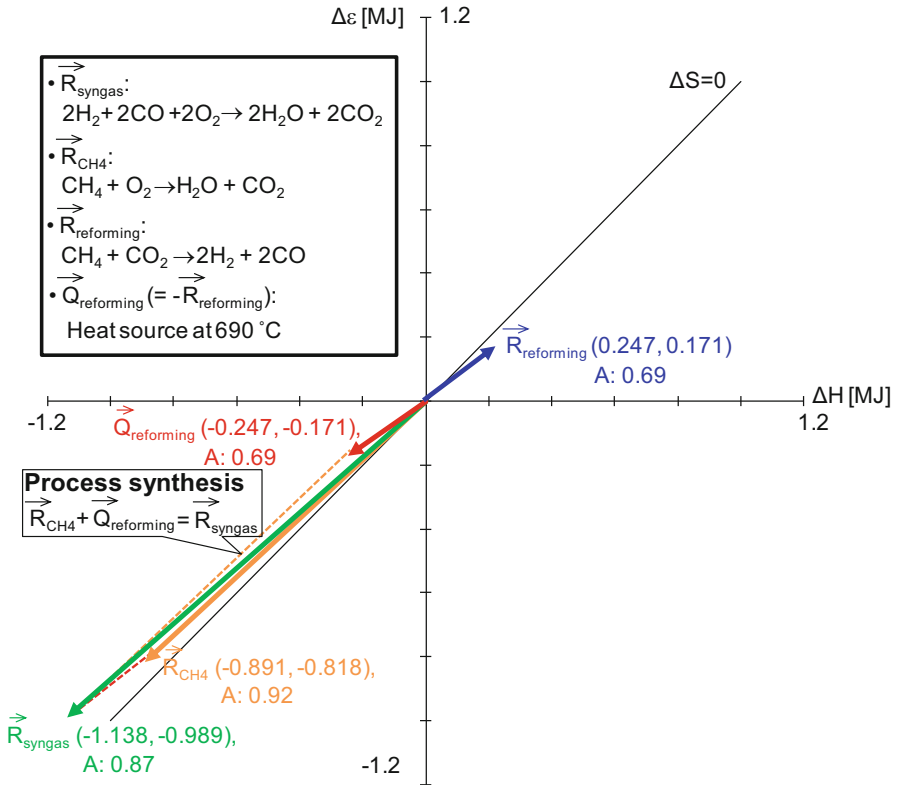
$$\vec{R}_{syngas}$$
$$2H_2 + 2CO + 2O_2 \rightarrow 2H_2O + 2CO_2 \tag{20}$$
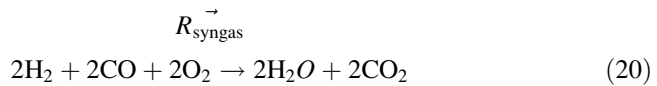
$$(\Delta H, \Delta \varepsilon) = (-1.137, -0.989) \tag{21}$$

$$A = 0.86 \tag{22}$$

Here, $\vec{R}_{CH4}$ and $\vec{R}_{syngas}$ indicate vectors of the perfect combustion reaction of CH_4 and syngas. Figure 6 expresses the relationship of $\vec{R}_{CH4}$, $\vec{R}_{syngas}$, $\vec{R}_{reforming}$, and $\vec{Q}_{reforming}$ on the thermodynamic compass. Here, the following equation is established:

$$R_{\text{CH4}}^{\rightarrow} - R_{reforming}^{\rightarrow} = R_{\text{syngas}}^{\rightarrow} \tag{23}$$

From Eq. (16) and Eq. (23),

$$R_{\text{CH4}}^{\rightarrow} + Q_{reforming}^{\rightarrow} = R_{\text{syngas}}^{\rightarrow} \tag{24}$$

As discussed earlier, dry reforming means the conversion of the chemical energy of CH_4 and thermal energy of a heat source to chemical energy of syngas. As shown in Fig. 6, the energy level of the heat source (0.69) is upgraded to that of the syngas (0.86). In other words, the exergy of thermal energy is recuperated in the form of syngas chemical energy. This exergy recuperation method can achieve a high degree of energy recovery.

Next, the application of PCM to the dry-reforming heat source will be considered. Figure 7 shows the thermodynamics compass of dry reforming as a target
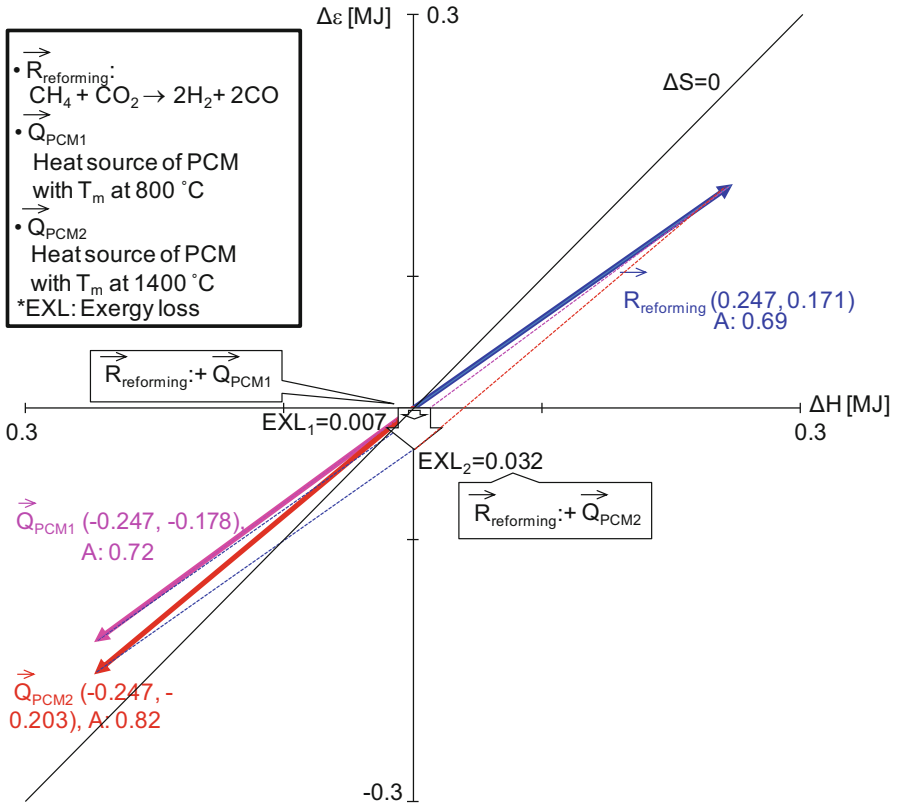

Fig. 7 Thermodynamics compass of dry reforming as a target process and heat source using PCM as a support process

process, and the PCM heat source as a support process. PCM is a heat source at a constant temperature (T_m); therefore, the energy level can be expressed by Eq. 3. In this study, two PCMs were assumed. PCM1 had T_m at 800 °C and PCM2 had T_m at 1400 °C. The vectors and energy levels can be expressed as follows:

$$\vec{Q}_{PCM1}$$
$$(\Delta H, \Delta \varepsilon) = (-0.247, -0.178) \tag{25}$$
$$T_m = 800°C, A = 0.72 \tag{26}$$
$$\vec{Q}_{PCM2}$$
$$(\Delta H, \Delta \varepsilon) = (-0.247, -0.203) \tag{27}$$

$$T_m = 1400°C, \ \ A = 0.82 \tag{28}$$

As shown in Fig. 7, the exergy loss of the system can be reduced by the energy level of PCM being closer to that of dry reforming. This means that the PCM selected is quite important for the efficient use of exergy. In other words, to decrease exergy loss, the T_m of the PCM should be as close as possible to the equilibrium temperature of the reaction, and two solutions should be considered to minimize the exergy loss. First is improvement of the heat transfer characteristic of the PCM. This will be lower than the temperature difference between PCM and reaction temperature, as the driving force of heat transfer. Because a marked increase in the heat transfer area is needed, a conventional shell-and-tube, or packed-bed type could not satisfy the need. Recently, microencapsulated PCM with diameter of about 40 μm, using Al-25 wt%-Si as PCM, was reported by Nomura et al. (2015b). The microencapsulated PCM has the potential to increase the heat transfer area remarkably. Second, is the development of catalytic PCM capsule. The reaction rate can be improved and the reaction temperature made close to the equilibrium temperature by using catalytic PCM. Catalytic PCM capsules with an Ni shell were reported by Maruoka and Akiyama (2006); however, there are few studies about these materials.

In summary, the development of catalytic microencapsulated PCM will be important for the development of future LHS technology.

6 Conclusions

This article described the recent advances in the use of LHS for high-temperature (over 100 °C) applications, with respect to each type of PCM (sugar alcohols, molten salt, and metal alloys). Table 4 gives a summary of the status of LHS development. The establishment of a high-temperature LHS technology is expected, because the temperatures of heat utilization systems are expected to increase.

Table 4 Status of LHS development

Material		Sugar Alcohol		Molten Salt		Alloy
		Conventional	Future	Conventional	Future	Future
Melting point [°C]		<120	150~	200 ~ 400	500~	500~
PCM candidate		Erythirol (T_m: 118 °C)	Mannitol (T_m: 167 °C)	NaNO$_3$ (T_m: 307 °C)	NaCl (T_m: 800 °C)	Al-12 wt%Si (T_m: 580 °C)
Performance	Heat capacity	High (340 kJ/kg)	High (330 kJ/kg)	Middle (182 kJ/kg)	High (483 kJ/kg)	High (504 kJ/kg)
	Thermal conductivity	Low (0.734 Wm^{-1}K^{-1})	Low	Low (0.561 Wm^{-1}K^{-1})	Low (1.26 Wm^{-1}K^{-1})	High (167 Wm^{-1}K^{-1})
	Corrosion	◎	◎	○	△ (under development)	× (under development)

References

Acem, Z., Lopez, J., Del Barrio, E.P.: $KNO_3/NaNO_3$–graphite materials for thermal energy storage at high temperature: part I.–elaboration methods and thermal properties. Appl. Therm. Eng. **30**, 1580–1585 (2010)

Bayón, R., Rojas, E., Valenzuela, L., Zarza, E., León, J.: Analysis of the experimental behaviour of a 100 kW_{th} latent heat storage system for direct steam generation in solar thermal power plants. Appl. Therm. Eng. **30**, 2643–2651 (2010)

Gil, A., Oró, E., Peiró, G., Álvarez, S., Cabeza, L.F.: Material selection and testing for thermal energy storage in solar cooling. Renew. Energy. **57**, 366–371 (2013)

Guillot, S., Faik, A., Rakhmatullin, A., Lambert, J., Veron, E., Echegut, P., Bessada, C., Calvet, N., Py, X.: Corrosion effects between molten salts and thermal storage material for concentrated solar power plants. Appl. Energy. **94**, 174–181 (2012)

Hidaka, H., Yamazaki, M., Yabe, M., Kakiuchi, H., Ona, E.P., Hirano, S., Saitoh, T., Oya, M., Yamazaki, M.: Long-term supercooled thermal energy storage (thermophysical properties of disodium hydrogenphosphate 12H_2O). In: Energy Conversion Engineering Conference and Exhibit, 2000 (IECEC) 35th Intersociety: IEEE, pp. 1013–1018, Las Vegas, NV, USA (2000)

Ishida, M.: Thermodynamics Made Comprehensible. Nova Science Publishers, Inc., New York (2002)

Izquierdo-Barrientos, M., Sobrino, C., Almendros-Ibáñez, J.: Thermal energy storage in a fluidized bed of PCM. Chem. Eng. J. **230**, 573–583 (2013)

Japan Society of Thermopysical property: Handbook of Thermal Analysis (Sinpen Netsubunseki Handbook in Japanese). Yokendou, Tokyo (2008)

Kaizawa, A., Kamano, H., Kawai, A., Jozuka, T., Senda, T., Maruoka, N., Akiyama, T.: Thermal and flow behaviors in heat transportation container using phase change material. Energy Convers. Manag. **49**, 698–706 (2008a)

Kaizawa, A., Maruoka, N., Kawai, A., Kamano, H., Jozuka, T., Senda, T., Akiyama, T.: Thermophysical and heat transfer properties of phase change material candidate for waste heat transportation system. Heat Mass Transf. **44**, 763–769 (2008b)

Kakiuchi, H., Yamazaki, M., Yabe, M., Chihara, S., Terunuma, T., Sakata, Y., Usami, T.: A study of erythritol as phase change material. IEA Annex. **10**, 11–13 (1998)

Kenisarin, M.M.: High-temperature phase change materials for thermal energy storage. Renew. Sust. Energ. Rev. **14**, 955–970 (2010)

Kojima, Y., Matsuda, H.: New PCMs prepared from erythritol-polyalcohols mixtures for latent heat storage between 80 and 100° C. J. Chem. Eng. Jpn. **37**, 1155–1162 (2004)

Kotzé, J.P., Von Backström, T., Erens, P.: Simulation and testing of a latent heat thermal energy storage unit with metallic phase change material. Energy Procedia. **49**, 860–869 (2014)

Laing, D., Bahl, C., Bauer, T., Lehmann, D., Steinmann, W.D.: Thermal energy storage for direct steam generation. Sol. Energy. **85**, 627–633 (2011)

Liu, M., Saman, W., Bruno, F.: Review on storage materials and thermal performance enhancement techniques for high temperature phase change thermal storage systems. Renew. Sust. Energ. Rev. **16**, 2118–2132 (2012)

Maruoka, N., Akiyama, T.: Exergy recovery from steelmaking off-gas by latent heat storage for methanol production. Energy. **31**, 1632–1642 (2006)

Mathur, A., Kasetty, R., Oxley, J., Mendez, J., Nithyanandam, K.: Using encapsulated phase change salts for concentrated solar power plant. Energy Procedia. In: Proceedings of Solar PACES, pp. 17–20, Las Vegas, NV, USA (2013)

Nomura, T., Okinaka, N., Akiyama, T.: Technology of Latent Heat Storage for high temperature application: a review. ISIJ Int. **50**, 1229–1239 (2010)

Nomura, T., Zhu, C., Sagara, A., Okinaka, N., Akiyama, T.: Estimation of thermal endurance of multicomponent sugar alcohols as phase change materials. Appl. Therm. Eng. **75**, 481–486 (2015a)

Nomura, T., Sagara, A., Zhu, C., Okinaka, N., Akiyama, T.: Heat storage performance of Al-base alloy as phase change material (In Japanese). In: Proceeding of 51th National Heat Transfer Symposium of Japan, Hamamatsu, Japan, May/21-23 (2014)

Nomura, T., Zhu, C., Sheng, N., Saito, G., Akiyama, T.: Microencapsulation of metal-based phase change material for high-temperature thermal energy storage. Sci. Rep. **5**, 9117 (2015). https://doi.org/10.1038/srep091171

Oya, T., Nomura, T., Tsubota, M., Okinaka, N., Akiyama, T.: Thermal conductivity enhancement of erythritol as PCM by using graphite and nickel particles. Appl. Therm. Eng. **61**, 825–828 (2013)

Pacheco, J.E., Showalter, S.K., Kolb, W.J.: Development of a molten-salt thermocline thermal storage system for parabolic trough plants. Transaction-American Society of Mechanical Engineers Jounal of Solar Energy Engineering. **124**, 153–159 (2002)

Pincemin, S., Olives, R., Py, X., Christ, M.: Highly conductive composites made of phase change materials and graphite for thermal storage. Sol. Energy Mater. Sol. Cells. **92**, 603–613 (2008)

Rellso, S., Delgado, E.: Experience with molten salt thermal storage in a commercial parabolic trough plant. ANDASOL-1 Commissioning and Operation. In: SolarPACES, Berlin, Germany (2009)

Sagara, A., Nomura, T., Tsubota, M., Okinaka, N., Akiyama, T.: Improvement in thermal endurance of D-mannitol as phase-change material by impregnation into nanosized pores. Mater. Chem. Phys. **146**, 253–260 (2014)

Tsutsumi, A.: Advanced IGCC/IGFC using exergy recuperation technology. CCT J. **11**, 17–22 (2004)

Tsutumi, A., Yoshida, K.: Exergy engineering. Kyoritsu syuppan, Tokyo (1999)

Yamagishi, Y., Takeuchi, H., Pyatenko, A.T., Kayukawa, N.: Characteristics of microencapsulated PCM slurry as a heat transfer fluid. AICHE J. **45**, 696–707 (1999)

Zhang, G., Li, J., Chen, Y., Xiang, H., Ma, B., Xu, Z., Ma, X.: Encapsulation of copper-based phase change materials for high temperature thermal energy storage. Sol. Energy Mater. Sol. Cells. **128**, 131–137 (2014)